Water Research 188 (2021) 116575

Contents lists available at ScienceDirect

Water Research

journal homepage: www.elsevier.com/locate/watres

Addition of a carbon fiber brush improves anaerobic digestion compared to external voltage application

Gahyun Baek[a], Pascal E. Saikaly[b], Bruce E. Logan[a,*]

[a] Department of Civil and Environmental Engineering, The Pennsylvania State University, 231Q Sackett Building, University Park, PA 16802, USA
[b] Biological and Environmental Science and Engineering Division, Water Desalination and Reuse Research Center, King Abdullah University of Science and Technology, Thuwal, Saudi Arabia

ARTICLE INFO

Article history:
Received 3 September 2020
Revised 11 October 2020
Accepted 26 October 2020
Available online 26 October 2020

Keywords:
Anaerobic digestion
carbon brush
microbial community structure
microbial electrolysis cell
surface area

ABSTRACT

Two methods were examined to improve methane production efficiency in anaerobic digestion (AD) based on adding a large amount of surface area using a single electrically conductive carbon brush, or by adding electrodes as done in microbial electrolysis cells (MECs) to form a hybrid AD-MEC. To examine the impact of surface area relative to electrodes, AD reactors were fitted with a single large brush without electrodes (FB), half a large brush with two electrodes with an applied voltage (0.8 V) and operated in closed circuit (HB-CC) or open circuit (HB-OC) mode, or only two electrodes with a closed circuit and no large brush (NB-CC) (equivalent to an MEC). The three configurations with a half or full brush all had improved performance as shown by 57-82% higher methane generation rate parameters in the Gompertz model compared to NB-CC. The retained biomass was much higher in the reactors with large brush, which likely contributed to the rapid consumption of volatile fatty acids (VFAs) and therefore improved AD performance. A different microbial community structure was formed in the large-size brushes compared to the electrodes. *Methanothrix* was predominant in the biofilm of large-size carbon brush, while *Geobacter* (anode) and *Methanobacterium* (cathode) were highly abundant in the electrode biofilms. These results demonstrate that adding a high surface area carbon fiber brush will be a more effective method of improving AD performance than using MEC electrodes with an applied voltage.

1. Introduction

Anaerobic digestion (AD) is an efficient method to degrade organic matter in wastewaters and produce methane but the process can require long hydraulic retention times for stable performance. The syntrophic relationship between fatty acid-degrading bacteria and methanogens is often considered as the rate-limiting step for soluble organic acid conversion to methane (Baek et al., 2018). Therefore, methane generation rates can be improved by reducing the background concentrations of volatile fatty acids (VFAs) produced from fermentation. Inserting electrodes like those used in a microbial electrolysis cell (MEC) into AD (i.e. AD-MEC), and applying a voltage to generate an electrical current and hydrogen gas, has been proposed to improve overall AD performance (Vu et al., 2020; Zhao et al., 2016). AD-MEC systems use exoelectrogenic bacteria on the anode to oxidize organic matter and reduce VFA concentrations, and the cathode can improve methane production either through electromethanogenesis ($8H^+ + 8e^- + CO_2 \rightarrow CH_4 + 2H_2O$) or by providing H_2 for hydrogenotrophic methanogenesis ($4H_2 + CO_2 \rightarrow CH_4 + 2H_2O$) (Cheng et al., 2009; Yu et al., 2018). AD-MEC systems have therefore been shown to increase methane production and organic removal efficiencies (Feng et al., 2015; Zhang et al., 2013; Zhao et al., 2016).

The main function of the electrodes in an AD-MEC has not been clearly distinguished between improvements due to additional surface area for biomass retention, and benefits of electrochemical processes that can remove additional organics and produce hydrogen gas. The operation of homogenized and continuously-fed AD reactors is dependent on the retention of biomass, especially methanogens (Choong et al., 2018). Adding supporting media with a high surface area into reactors has therefore been used to ensure a high biomass concentration (Show and Tay, 1999). Most of the materials used for bioelectrodes in AD-MECs provide a relatively high surface area compared to controls without electrodes. Carbon felt or carbon cloth materials have porous structures which could benefit AD performance by retaining biomass and preventing washout, in addition to stimulating electrochemical reactions.

* Corresponding author.
E-mail address: blogan@psu.edu (B.E. Logan).

https://doi.org/10.1016/j.watres.2020.116575
0043-1354/

Despite of the importance of this surface area effect, the electrode packing density (i.e. electrode surface area to reactor volume ratio) has not been well documented or specifically examined in AD-MEC studies. Electrode packing densities have varied over a wide range in AD-MEC studies, from 0.7 to 15.1 m^2/m^3 of reactor volume, which could have impacted AD performance even without current production (Baek et al., 2020; Cai et al., 2016; De Vrieze et al., 2014; Feng et al., 2015; Liu et al., 2016; Vu et al., 2020). Low electrode packing densities (<1 m^2/m^3) would not be expected to impact methane production rates by more than a small amount (0.6–1.2%) due to a small percentage of the substrate being used for current generation relative to that for overall methane production (Baek et al., 2020; Feng et al., 2015). However, AD-MEC systems with a relatively small amount of current through the circuit have shown to achieve higher or more stable AD performance than conventional AD systems (Baek et al., 2020). In addition to increasing surface area available for microorganisms, the use of electrically conductive materials can also provide a beneficial platform for direct interspecies electron transfer (DIET) between electroactive bacteria and methanogens even in the absence of current generation (Baek et al., 2015; Cruz Viggi et al., 2014; Li et al., 2015). Through DIET, the electrons from organic oxidation can be transferred directly toward methanogens without redox intermediate (i.e. hydrogen), which could make the AD process more efficient and contribute to enhanced methane generation rates (Baek et al., 2018).

In this study, we investigated the impact of surface area relative to current generation using electrodes by adding carbon fiber brushes of different sizes into AD reactors. We hypothesized that the large surface area provided by the brushes was more critical to AD performance than current generation using smaller-size MEC electrodes. Carbon brushes were chosen for these tests because they provide a very high surface area-to-volume ratio, and the open brush structure has advantages of less potential for clogging compared to other carbon-based woven materials (e.g., pieces of carbon felt or carbon cloth) (Logan et al., 2007). In addition, the potential for DIET is enhanced by using carbon brushes due to their high electrical conductivity (650 S/cm for brushes used here). This strategy to add brushes into AD provide additional advantages compared to adding particles to stimulate DIET (e.g., magnetite, carbon nanotube, activated carbon) (Baek et al., 2015; Li et al., 2015; Liu et al., 2012) because there is no possibility of material washout using the brushes compared to particles. The impact of large carbon brushes on methane generation rates and COD removal rates was examined by adding brushes that filled, or half-filled the reactor volume compared to reactors with two smaller-size brush electrodes in the presence and absence of current production. The amount of attached biofilm to these different brushes was quantified in terms of protein, with the contribution of current generation evaluated in terms of coulombic efficiency and total internal resistances based on the electrode potential slope (EPS) method (Cario et al., 2019). To obtain a more comprehensive insight into process performance, the microbial communities on the brushes and in suspension were characterized using Illumina sequencing of both active (16S rRNA) and total (16S rRNA gene) microbial populations.

2. Materials and methods

2.1. Inoculum and substrate

Sludge was collected from the anaerobic digester at the Pennsylvania State University wastewater treatment plant and used as the inoculum. The sludge was sieved using a screen (mesh size of 850 μm) to remove large particles that lead to clogging of the sampling port and obtain a homogenous inoculum, and then stored at 4°C. Before utilization as an inoculum, the sludge was held for 24 h at 35°C to activate microorganisms and decrease concentrations of easily degraded biodegradable organic matter. The sludge composition was: total chemical oxygen demand (TCOD) of 22,500 ± 500 mg/L, soluble COD (SCOD) of 540 ± 30 mg/L, total suspended solids (TSS) of 19,000 ± 700 mg/L, and a volatile suspended solid (VSS) of 14,800 ± 400 mg/L. A synthetic substrate used for AD tests was prepared with glucose as the sole carbon source (2.5 g/L) in 100 mM phosphate buffer solution (PBS) containing 4.9 g/L $NaH_2PO_4 \bullet H_2O$, 9.2 g/L Na_2HPO_4, 0.6 g/L NH_4Cl, 0.3 g/L KCl, mineral (12.5 mL/L) and vitamin (5 mL/L) solutions (pH =7.1, conductivity = 12.1 mS/cm) (Cheng et al., 2009). The concentration of PBS solution was changed from 50 to 100 mM from the third batch cycle since a low pH (6.6–6.7) was measured at the end of the second batch cycle.

2.2. Preparation of brushes and reactor configurations

Two large brushes were used to provide high surface areas for microbial growth and two smaller brushes were used as electrodes for the four different reactor conditions (Fig. 1). The full-size brush (6 cm long and 4 cm in diameter), half-size brush (3 cm long and 4 cm in diameter) and small-size anode brush (1 cm long and 1.5 cm in diameter) were made from carbon fibers wound into two twisted titanium wires (Mill-Rose). The bristles for the carbon brushes were 0.00072 mm in diameter and had an electrical conductivity of 650 S/cm (zoltek.com/products/px35). The carbon brushes were heat treated at 450°C for 30 min before use. Stainless steel (SS) brushes used for the cathodes had the same length and diameter as the anodes, but the bristles were 0.005 cm in diameter.

The AD reactors (duplicates for each test condition) were glass bottles filled with 270 mL of liquid and they had 60- or 80-mL of headspace (two different bottle types). The bottles were sealed with a rubber stopper held on with a screw cap. AD reactors were tested with four different configurations: a full-size brush with no electrodes (FB), a half-size brush to provide a high surface area along with two electrodes either with an applied voltage of 0.8 V (HB-CC) or with an open circuit (HB-OC), or only the electrodes and no large brush operated with an applied voltage of 0.8 V to simulate AD with MEC (NB-CC) (Fig. 1). The FB reactor was used to show the maximum possible impact of conductive surface area on AD performance, while the NB-CC condition represented AD-MECs with low electrode packing density as used in several previous studies (Baek et al., 2020; Feng et al., 2015). The HB-CC configuration was examined as a possible method to improve AD using both approaches (i.e., current generation and adding a large surface area). HB-OC configuration was used as a control to provide same surface area as HB-CC but remove the impact of current generation on performance. To prevent short circuiting in the reactors with the half brush between the brush and electrodes a piece of insulative rubber was installed at the bottom of the electrodes by piercing the titanium tip into the rubber (Fig. 1C). The tip was sealed by epoxy treatment to make it be electrically insulated.

The surface area of brushes was calculated for all reactor configurations based on the bristle geometry of each carbon and SS brushes (Table 1). The cylindrical area was calculated as $A_c = 2\pi r (r + h)/V$, where h is the height and r is the radius of the brush, and V is the liquid volume. The specific bristle area for carbon brushes was calculated as $A_s = 2\pi r_b n (r_b + r)/V$, where r_b is the radius of bristle (0.00036 cm) and n is the total number of bristles (400,000 bristles per inch). The specific bristle area for SS brush was estimated as $A_s = 2m/r_b \rho V$, where m is the total mass of the bristles and ρ is the density of the SS fiber.

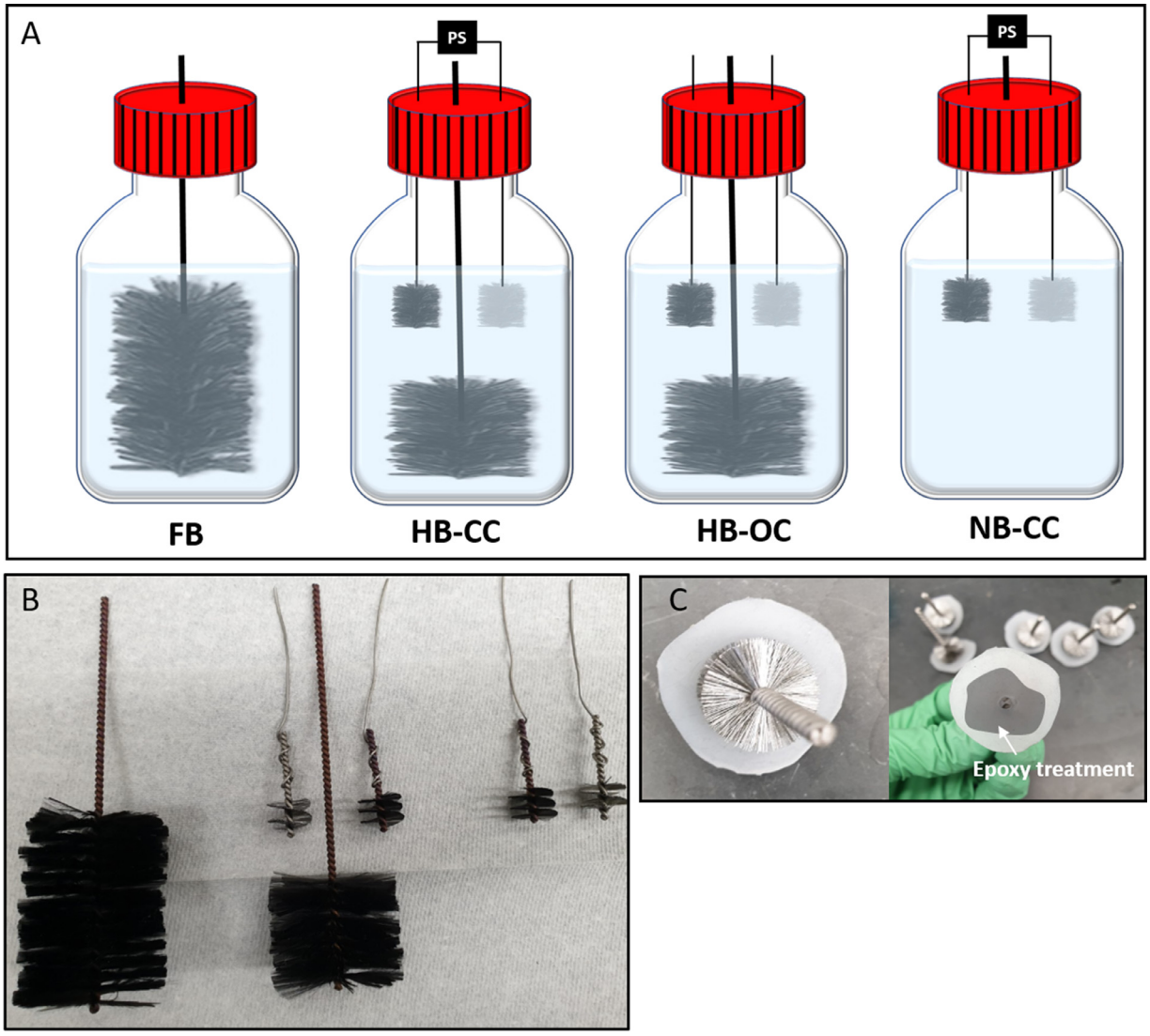

Fig. 1. (A) Schematics of the four AD reactor configurations, (B) photographs of the brushes used for applying voltage or providing surface area for microbial attachment, and (C) photographs of the non-conductive plates added to the HB-CC and HB-OC reactor electrodes to prevent short circuiting.

Table 1
Normalized surface area of brushes and electrodes.

Calculation basis	FB	HB-CC	HB-OC	NB-CC
Cylindrical area (A_c) of all brushes/working volume (m^2/m^3)	37.2	29.4	29.4	6.1
Cylindrical area (A_c) of electrodes/ working volume (m^2/m^3)	-	6.1	-	6.1
Specific bristle area (A_s) of all brushes/ working volume (m^2/m^3)	1580	890	890	100
Specific bristle area (A_s) of electrodes/ working volume (m^2/m^3)	-	100	-	100

2.3. Repeated batch operation

For the first cycle, a glucose medium with 20% (v/v) of inoculum was used producing a final glucose concentration of 2.5 g/L. The reactors were operated under fed-batch mode by replacing 50% of the liquid with fresh medium at the end of each cycle. Before starting each batch cycle the reactor liquid was sparged with pure nitrogen gas for 3 min. The duration of the cycle was defined based on the end of gas production or a low electrical current from all reactors. A fixed external voltage of 0.8 V between two electrodes was applied to the NB-CC and HB-CC reactors using a potentiostat (VMP3, BioLogic, Knoxville, TN), consistent with applied voltages used in previous tests to enhance AD efficiency (Ding et al., 2016; Vu et al., 2020). The FB reactor did not contain electrodes, and the HB-OC reactors were operated under open circuit conditions. Biogas was collected by gas collection bag (Cali-5-Bond, Calibrated Instruments, NY) and liquid samples were collected from the middle of the reactors through sampling ports. All AD reactors were operated in duplicate and in a temperature-controlled room at 35°C. The current was recorded at 10 min intervals using a potentiostat (VMP3, BioLogic, Knoxville, TN).

2.4. Protein assay

The attached and suspended biomass were quantified based on total protein concentration using a bicinchoninic acid (BCA) protein assay kit (Sigma Aldrich) following previously described procedures (Bond and Lovley, 2003; Ishii et al., 2008; Rossi et al., 2018).

For the extraction of the attached biomass, the pieces of brushes were cut with sterile scissors and placed in a petri dish with 5 mL (small brushes) or 10-mL (large brushes) of 0.2 N NaOH. The 1-h extraction was performed by withdrawing and re-adding the NaOH solution several times over the surface of brushes (15 min of intervals) using a pipette to improve protein extraction. The resulting solution was removed and weighed. An equal amount of deionized water was used for further rinsing the brushes to collect any remaining solution. The liquids were pooled together, yielding a sample containing 0.1 N NaOH. For suspended biomass, 10 mL of mixed liquor was centrifuged (13,000 × g, 3 min), the suspension was discarded, and pellet was re-suspended in 0.1 N NaOH. The pretreated samples (both attached and suspended biomass) were frozen (–20°C) followed by thawing at 100°C for 10 min, and this freeze-thaw cycle was repeated three times. Then, the sample was centrifuged (13,000 × g, 3 min) to remove any cell debris. The protein concentration was quantified by the BCA method against a bovine serum albumin standard (Bond and Lovley, 2003). The measured protein was normalized by the weight of used brushes (for attached biomass) or the volume of used suspension (for suspended biomass). Total protein in each reactor was presented by multiplying by total weight of brushes or total working volume of the reactor.

2.5. Nucleic acid extraction, library preparation, amplicon sequencing, bioinformatics processing, and statistical analysis

The attached and suspended biomass samples were collected at the end of the third batch cycle from each reactor. DNA extraction was performed using the standard protocol for FastDNA Spin kit for Soil (MP Biomedicals, USA) and RNA was extracted using the standard protocol for RNeasy PowerMicrobiome Kit (Qiagen, Germany) and reverse-transcribed using 2X Platinum SuperFi RT-PCR Master Mix from the SuperScript IV One-Step RT-PCR System (Thermo Fisher Scientific, USA). 16S rRNA gene region V4 sequencing libraries were prepared according to the Illumina protocol by using the forward (515F) and reverse (806R) tailed primers (Apprill et al., 2015; Illumina, 2015). The purified sequencing libraries were pooled and paired-end sequenced (2 × 300 bp) on a MiSeq (Illumina, USA). The trimmed and merged reads were dereplicated, formatted for use in the UPARSE workflow, and then clustered using the USEARCH v. 7.0.1090. The OTU abundances were estimated using the USEARCH v. 7.0.1090 and the taxonomy was assigned using the RDP classifier. The detailed information about nucleic acid extraction, library preparation, amplicon sequencing, and bioinformatics processing is provided in the Supporting information. The sequences obtained in this study were deposited in the NCBI Sequence Read Archive under the bioproject accession number PRJNA658582.

2.6. Measurements and calculations

The gas composition in the headspace was analyzed with a gas chromatograph (GC) using 250 μL of gas extracted from the gas collection bag using an airtight gas syringe (Hamilton, Reno, NV, USA). Hydrogen and methane were analyzed using a GC (model 2601B, SRI Instrument, Torrance, CA, USA) equipped with a 3-m Molsieve 5A 80/100 column (Altech Associates, Inc., Bannockburn, IL) and thermal conductivity detector (TCD; a detection limit of 0.01%) with argon as the carrier gas. Carbon dioxide was analyzed using another GC (model 310, SRI Instrument, Torrance, CA, USA) with a 1-m silica gel column (Restek, Bellefonte, PA, USA) and TCD (a detection limit of 0.01%) with helium as the carrier gas. The methane volume was calculated as $V_{m,\,t} = V_{g,\,t}\ f_{m,\,t} + V_h\ (f_{m,\,t} - f_{m,\,t-1})$, where $V_{g,\,t}$ is biogas volume in gas bag and $V_{m,\,t}$ is methane volume measured at time t (mL), f_m is the fraction of the methane in biogas, and V_h is the headspace volume (mL) of the reactor (Trzcinski and Stuckey, 2012). The volume was corrected to standard condition (0°C and 1 atm). Soluble chemical oxygen demand (SCOD) was analyzed using standard methods (TNTplus COD reagent; HACH company). Volatile fatty acids (VFAs; acetate, propionate, and butyrate) were quantified using a GC (Shimadzu, GC-2010 Plus, Japan) equipped with a Stabilwax-DA column (30 m × 0.32 mm × 0.5 μm, Restek, Bellefonte, PA) and flame ionization detector (FID; a detection limit of each VFA of 0.1 mM) with nitrogen as the carrier gas. The samples for SCOD and VFA measurement were prepared by using a syringe filter with 0.45 μm of pore size. The total and suspended solid concentrations were measured according to a standard method (Association et al., 1920). All chemical analyses were performed in duplicate.

The coulombic efficiency (CE) was calculated as $CE = C_t/C_c$, where C_t is the total coulombs calculated by integrating the current over time, and C_c is the total charge consumed based on the SCOD removal. The contribution of current generation to methane production was estimated by the ratio of the theoretical methane production from current to total methane production as $r_{th/tot} = W_E/W_{CH4}$, where W_E is the electrical energy input and W_{CH4} is the energy content of the methane produced. The methane generation rate over time was fitted using the Gompertz equation to interpret the experimental results and directly compare each parameter among the different reactor configurations (Baek et al., 2015):

$$M(t) = P\ exp\left[-exp\left\{\frac{R_m\ e}{P}(\lambda - t) + 1\right\}\right]$$

where $M(t)$ is the accumulated methane production at time t, R_m is the maximum methane production rate (mL/d), P is the maximum methane potential (mL), e is Euler's constant (2.718), and λ is the lag phase length (d).

Total internal resistance can be obtained using polarization data obtained by applying voltage step-by-step with an interval as done in a previous study (Cario et al., 2019) or by using linear sweep voltammetry (Kang et al., 2017; Nam et al., 2017). Here, the polarization data were obtained by reducing the applied voltage from 0.8 V to 0.2 V, at 0.1 V intervals, with 20 min at each applied voltage. Current was recorded at 1-min intervals with the last five minutes averaged and used for polarization curve. The electrode potential slope (EPS) method was used to obtain the total internal resistance of the HB-CC and NB-CC. For the EPS method the whole-cell potentials were plotted with the potential on the y-axis and the current density on the x-axis. The linear portion was fitted by $E = mi + b$, where i is the current density (A/m^3), the slope m is defined as the total internal resistance (mΩ/m^3), and the y-intercept was open circuit potential of the cells.

3. Results & discussion

3.1. Methane production and COD removal

After successful biofilm acclimation cycles (Fig. S1) the reactors with the high-surface area brushes produced methane faster than the reactor containing only the MEC electrodes (NB-CC) (Fig. 2A). Methane production during the third batch cycle showed the lowest accumulated volume for the NB-CC reactor (208 ± 24 mL) and the highest gas volume for the FB reactor (249 ± 2 mL). The three configurations with the full or half brushes all showed similar overall trends in gas production, with similar final methane volumes (235–249 mL). Despite of the presence of the electrodes in the NB-CC reactors, gas production was much less by the end of the cycle than that of the other reactors. There was negligible H_2

Table 2
The parameters estimated by modified Gompertz model.

Reactors	Maximum CH_4 potential (P, mL)	Maximum CH_4 production rate (R_m, mL/d)	Lag phase (λ, d)	R^2
FB	253 ± 16	69 ± 15	0.38 ± 0.33	0.9984
HB-CC	240 ± 22	59 ± 17	0.31 ± 0.48	0.9970
HB-OC	248 ± 15	63 ± 11	0.43 ± 0.30	0.9988
NB-CC	232 ± 63	38 ± 15	0.43 ± 0.92	0.9920

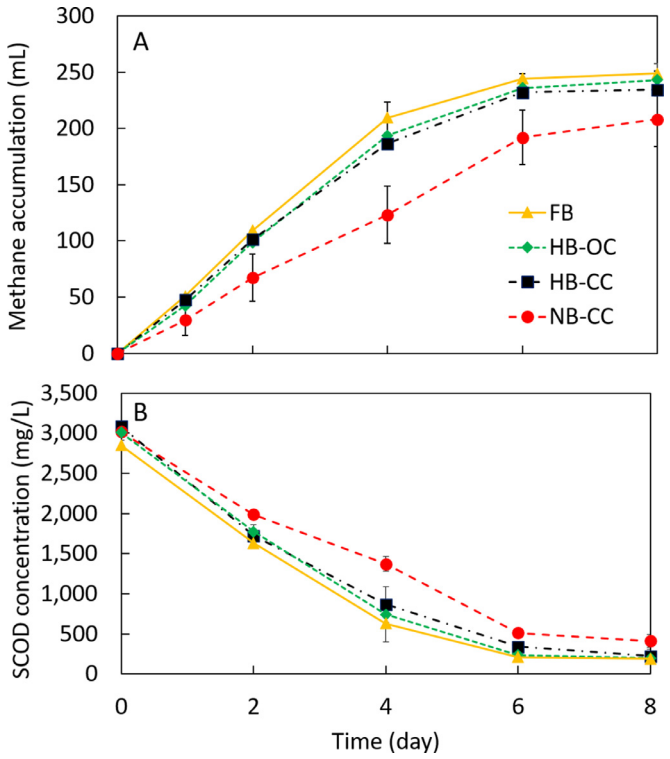

Fig. 2. (A) Methane accumulation and (B) soluble COD consumption profiles during the third batch cycle. For methane accumulation data of HB-CC, only one of the duplicates was shown due to substantial gas leakage from the other reactor.

production (< 0.2% in biogas) in all cycles and for all days except day 1, where acidogenesis mainly occurred in all reactors.

The performance of the different reactors in terms of methane production was consistent with parameters fitted to the modified Gompertz model (Table 2), with all results having R^2 >0.99. The three reactors with full or half brushes (FB, HB-CC and HB-OC reactors) had 3.7–9.0% higher values of the maximum methane potential (P) and 57–82% higher values in the maximum methane production rate parameter (R_m) compared to the NB-CC reactor. These higher rates with the large brush area indicated that the presence of the brush was more critical for methane production than electrodes in the AD reactors. The methane production estimated from the P values from the model agreed with the experimental data, indicating that the incubation period of the third cycle (i.e. 8 days) was enough to observe the difference in AD efficiency among the reactors. The estimated lag phase (λ) was similar and low for all reactors (0.31–0.43 days) indicating the microbial community was well acclimated for the fed-batch cycles.

The SCOD removals were consistent with methane production showing slower removal rates in the NB-CC bottles compared to the other reactors (Fig. 2B). The final SCOD removal at the end of the cycle was above 93% for the three reactors with the large brushes (93 ± 3%, FB, 93 ± 3%, HB-CC, and 94 ± 2%, HB-OC) compared to 86 ± 3% for the NB-CC reactors.

3.2. VFA production and removal

Total VFA concentrations were always lower in the AD reactors with the large brushes compared to the electrode-only NB-CC reactors (Fig. 3). Acetate, propionate and butyrate were the dominant acidogenic products from glucose fermentation consistent with previous reports (Lu et al., 2020; Qin et al., 2020). After the total VFA concentrations reached a maximum on day 2 with slight drop in pH from 6.9 to 6.4 (Fig. S2), more rapid conversion of butyrate to acetate was observed during days 2–4 in FB, HB-CC, and HB-OC, while butyrate remained on days 4 and 6 in NB-CC reactors. In addition, the propionate degradation rate was much slower in NB-CC, resulting in 175 mg as COD/L of propionate at the end of the cycle. The lower propionate accumulation in the reactors with large carbon brushes could have been due to enhanced syntrophic propionate oxidation by DIET stimulated by the presence of the electrically conductive surface area (Baek et al., 2018; Cruz Viggi et al., 2014). Having a carbon brush with large surface therefore could have improved AD because anaerobic propionate oxidation is a highly endergonic reaction ($\Delta G^{o'}$ = +76.1 kJ/mol). This speculation is supported by previous reports which observed DIET in both pure- and mixed-culture systems when electrically conductive carbon-based woven materials were added (Chen et al., 2014; Dang et al., 2016; Zhao et al., 2015).

3.3. Current production and its impact on performance

The reactors with the electrodes and no brush (NB-CC) showed better electrochemical performance than the HB-CC reactors with the large half-sized brush in terms of current density and *CE* values despite identical electrode configurations (Fig. 4A). Polarization data for the two reactors was similar, resulting in comparable slopes using the EPS method (Cario et al., 2019). The internal resistances of the two types of reactors calculated from the slopes were not appreciably different based on the overlap of the standard error of the slopes at lower current densities and applied voltages (96 ± 6 for HB-CC reactor and 93 ± 6 $m\Omega/m^3$ for NB-CC reactor) (Fig. 4B). However, for applied voltages above 0.5 V for the HB-CC reactors, and 0.7 V for NB-CC reactors, there was no increase in current density (Cario et al., 2019). At an applied voltage of 0.8 V (i.e. a set potential in this experiment), a 2.7-fold higher current was produced in NB-CC than HB-CC which explained their different performance and current densities in the constant applied voltage tests. The lower electrochemical performance for the HB-CC reactor was due to the presence of the large half-sized brush as this was the only difference between the HB-CC and NB-CC reactors. The presence of the half-sized brush resulted in a more rapid consumption of VFAs that are used for current generation, which could have explained the lower current density in the HB-CC reactors.

There was no appreciable difference in performance for the reactors with the half brush operated in either open circuit (HB-OC) or with current generation (HB-CC) due to an applied voltage, indicating that current production did not measurably influence overall AD rates (Figs. 2 and 3). In addition, current production alone (for the NB-CC reactor) resulted in reduced overall performance compared to the other reactors. Analysis of the fraction of the substrate removed on the basis of the coulombic efficiencies showed

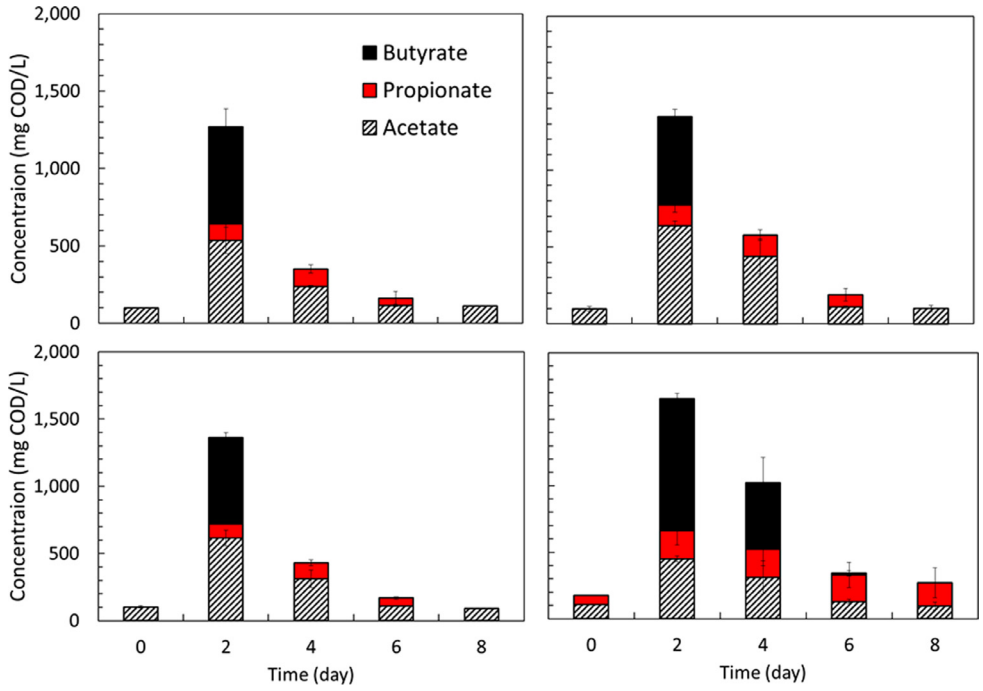

Fig. 3. Volatile fatty acid production and consumption profiles in (A) FB, (B) HB-CC, (C) HB-OC and (D) NB-CC during the third batch cycle.

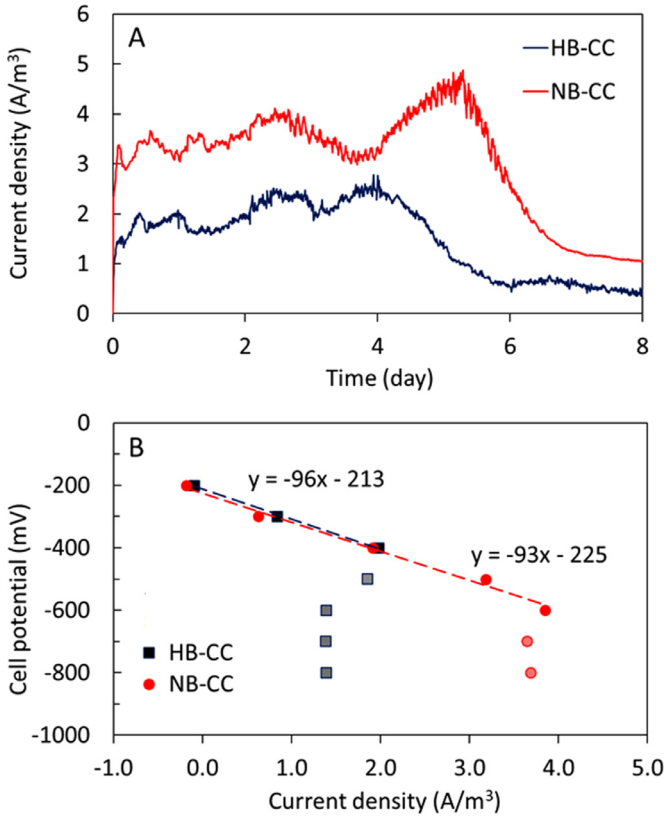

Fig. 4. (A) Current generation during the third batch cycle, and (B) whole-cell polarization curves for the HB-CC and NB-CC reactors. The faded color data points were not included in the linear fits.

that the closed circuit reactors had <7% of the substrate used by the anode bacteria, with *CE* values of 3.4% (HB-CC) and 6.9% (NB-CC). Thus, there was a negligible impact of current generation on performance.

The lack of an impact of current production on methane generation or COD removal rates was likely due to the small electrode packing density (6.1 m^2/m^3 as cylindrical area and 200 m^2/m^3 as specific bristle area). Higher electrode brush densities (63.0 m^2/m^3 as cylindrical area) produced a higher maximum current density (31.9 A/m^3) with same substrate type of medium (glucose at 2.5 g/L) (Vu et al., 2020) than those obtained in this study (2.7 A/m^3 for HB-CC and 4.9 A/m^3 for NB-CC). However, asshown by using a large brush in our studies the rates would be improved just due to the large surface area of the brush even in the absence of current production.

3.4. Biomass on brushes

Protein was measured on the brushes and in the mixed liquor of each reactor to compare biomass retention among the reactors (Fig. 5). The biomass measured for the half- (120–121 mg) and full-size (118 mg) brushes were similar and much higher than those on the small-size brushes (1–15 mg) or in the mixed liquor (6–57 mg). The amount of protein was 3.1–9.5-fold higher in the mixed liquor of NB-CC than other reactors presumably owing to the less surface area for the attached growth. The differences in suspended biomass concentrations among the reactors also could be visually observed based on less turbidity of solution for the reactors with large brushes than that of the NB-CC reactors without the large brushes (Fig. S3). The sum of protein was much higher in HB-OC (136 ± 5 mg), HB-CC (135 ± 1 mg), and FB (133 ± 1 mg) configurations compared to NB-CC (37 ± 2 mg), suggesting the biomass retention by the large surface area brushes was the crucial factor in AD performance of the reactors with the different configurations. The lack of a difference in total protein amount among FB, HB-CC, and HB-OC reactors suggests that the differences in brush shapes and materials could have impacted overall biomass retention on the brushes. Although the FB configuration provided twice as much surface area than HB reactors (HB-CC or HB-OC), the portion of active surface area which was favorable for microbial attachment might have not been much larger due to the inaccessibility of the inner parts of the brushes. Similar protein amounts among these

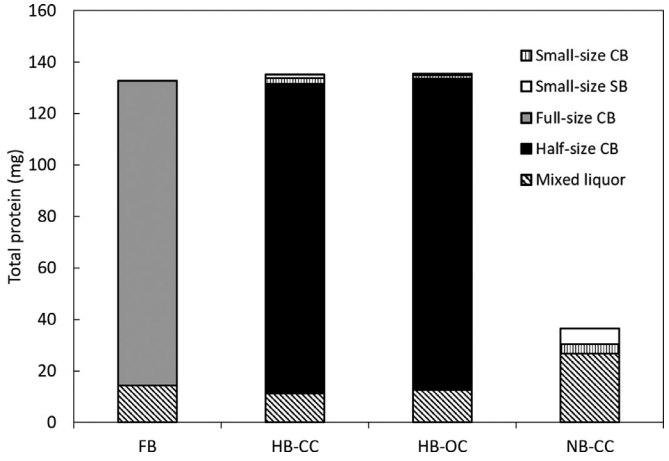

Fig. 5. Total protein measured on the brushes and mixed liquor for the different reactor configurations. The measured protein (mg/g brush or mg/L) was multiplied by the total weight of the brushes (for attached biomass) or total liquid volume of reactor (for suspended biomass). CB refers to carbon brush anode and SB refers to stainless steel brush cathode.

three reactors did seem to be in good agreement with the similar AD efficiencies of these three configurations (Fig. 2).

3.5. Spatial distribution of the microbial community

The biomass samples taken from different locations (biofilms on brushes and the solutions) were analyzed for both 16S rRNA gene and 16S rRNA to compare the total and active microbial community among the four reactors. A total of 584,971 (rRNA gene library) and 678,884 (rRNA library) non-chimeric, quality-filtered reads were obtained and they were clustered into 906 OTUs at 97% identity. The most abundant 20 OTUs in each sample were presented in a heatmap with their relative abundance and taxonomic classification at the genus and phylum level (Fig. 6).

The dominant methanogen family varied depending on the location of the biomass sampling. Based on 16S rRNA gene sequencing, the relative abundance of *Methanobacteriaceae* was much higher on the cathodes of the HB-CC (40%) and NB-CC (36%) reactors compared to the others (1–9%) (Fig. 7A) and most of them were assigned to the genus *Methanobacterium* (Fig. 6A). Although the relative abundance of this group decreased in 16S rRNA sequencing (Fig. 6B), *Methanobacteriaceae* was still the most predominant methanogenic family on the cathodes of the HB-CC and NB-CC reactors (Fig. 7B). This finding is consistent with previous studies on biocathodes of MECs or electromethanogenesis cells where the relative abundance of *Methanobacterium* was the highest among methanogens and they were mainly responsible for CH_4 production in H_2- or electrons-accepting conditions (Baek et al., 2017; Siegert et al., 2015; Zhen et al., 2016).

Methanotrichaceae was the predominant methanogen family on brushes which did not function as electrodes (i.e., small-size brushes in HB-OC and half- or full-size carbon brushes). Most of these methanogens were assigned to the genus *Methanothrix* (Fig. 6A), whose members are acetoclastic methanogens, although recently they were found to be capable of participating in DIET by converting CO_2 to CH_4 directly (Rotaru et al., 2014b). Given that their relative abundance was much higher in the 16S rRNA library, members of *Methanothrix* may have substantially contributed to the metabolic activity of methane production in brushes that did not function as electrodes. Although we did not conclusively show DIET here on the graphite fiber brushes, previous reports on DIET between *Methanothrix* and VFA-degrading partners has been shown by others using other electrically conductive materials (Liu et al., 2020a; Xu et al., 2020). *Methanomicrobiaceae* showed extremely low relative abundance (<0.04%) in 16S rRNA gene libraries while it increased significantly (1–17%) in 16S rRNA libraries for these brushes (Fig. 7). Their abundance was higher in solutions, consistent with a previous AD study which found that *Methanomicrobiaceae* were more abundant in solutions than biofilms on carbon cloth or biochar (De Vrieze et al., 2016).

Among the 41 known phyla classified from bacterial 16S rRNA gene and 16S rRNA sequences, *Firmicutes, Bacteroidetes*, and *Proteobacteria* were dominant in all samples although their relative abundance varied (Fig. 8). For example, *Proteobacteria* showed 3.1–6.2-fold higher relative abundance on the anodes than cathodes in both 16S rRNA gene and 16S rRNA libraries of the HB-CC and NB-CC reactors. However, there was negligible difference in the relative abundance of *Proteobacteria* between the small-size carbon brush and SS brush in the HB-OC reactor despite having the same reactor configuration as the HB-CC reactor. This suggests that the electron-producing or -accepting mechanism around the electrode developed a substantially different bacterial community from the community that developed on the brushes in the absence of current. *Chloroflexi* showed a higher relative abundance on the large carbon brush (7.7–8.5% in 16S rRNA gene- and 4.9–6.2% in 16S rRNA-libraries), with much lower abundances in the other samples. This is consistent with their reported role in DIET showing their dominance on conductive materials added into AD reactors (Baek et al., 2020; Feng et al., 2018). At the OTU level, OTU_2 which belonged to *Alistipes* was highly abundant in all mixed liquor samples (>27%) in the 16S rRNA gene library (Fig. 6). Although *Alistipes* has been reported in several AD reactors (Liu et al., 2020b; Sposob et al., 2020), it might not have made only a small contribution to the overall metabolic activities because their relative abundance in the 16S rRNA library was much lower. Some of the OTUs belonging to *Firmicutes* (e.g., OTU_1, 3, 4, and 6) were highly abundant in most of the samples and they likely were responsible for fermentation of glucose and production of VFAs (Feng et al., 2015; Lin et al., 2007). The OTU_10 which was classified into the genus *Geobacter* showed higher relative abundance only in the anode samples of HB-CC and NB-CC, with much greater abundance in 16S rRNA- (19.7–24.7%) than in 16S rRNA gene- (5.8–6.2%) libraries, indicating they are highly active members of the anodic community. The dominance of *Geobacter* at the anode in AD-MEC or MEC has been extensively reported due to their ability to export electrons directly to the anode (Yu et al., 2018). *Syntrophomonas* (OTU_16), known as syntrophic butyrate-oxidizing bacteria, was generally more abundant in the 16S rRNA library for the biomass samples obtained from the large-size brushes compared to the other brushes. This greater abundance could partially reflect recent reports on putative DIET between *Syntrophomonas* and *Methanothrix* in the presence of conductive materials (Zhao et al., 2018), considering the high relative abundance of *Methanothrix* here for the large-size brushes. Although there has been no direct evidence of DIET for *Syntrophomonas* species, their enrichment in DIET-stimulating condition has been frequently reported (Zhang et al., 2020; Zhao et al., 2018; Zhao et al., 2016).

There were some other dominant OTUs in brush biofilms without current which were affiliated with *Acetothermiia, Thermovirga, Victivallis*, and Candidatus *Cloacamonas*, all classified to be fermentative bacteria (Fig. 6) (Chen et al., 2018; Pampillón-González et al., 2017; Suarez et al., 2019; Zoetendal et al., 2003). In contrast, the microbial populations of the brushes functioning as electrodes were dominated only by several major groups, possibly due to the selective pressure regarding current production (Figs. 7 and 8). Not only for the fermentative bacteria, whole microbial communities were generally less diverse in electrode biofilms. This was shown by the two alpha diversity indices, the Shannon index which gives more weight to abundant OTUs, and the Chao1 index which con-

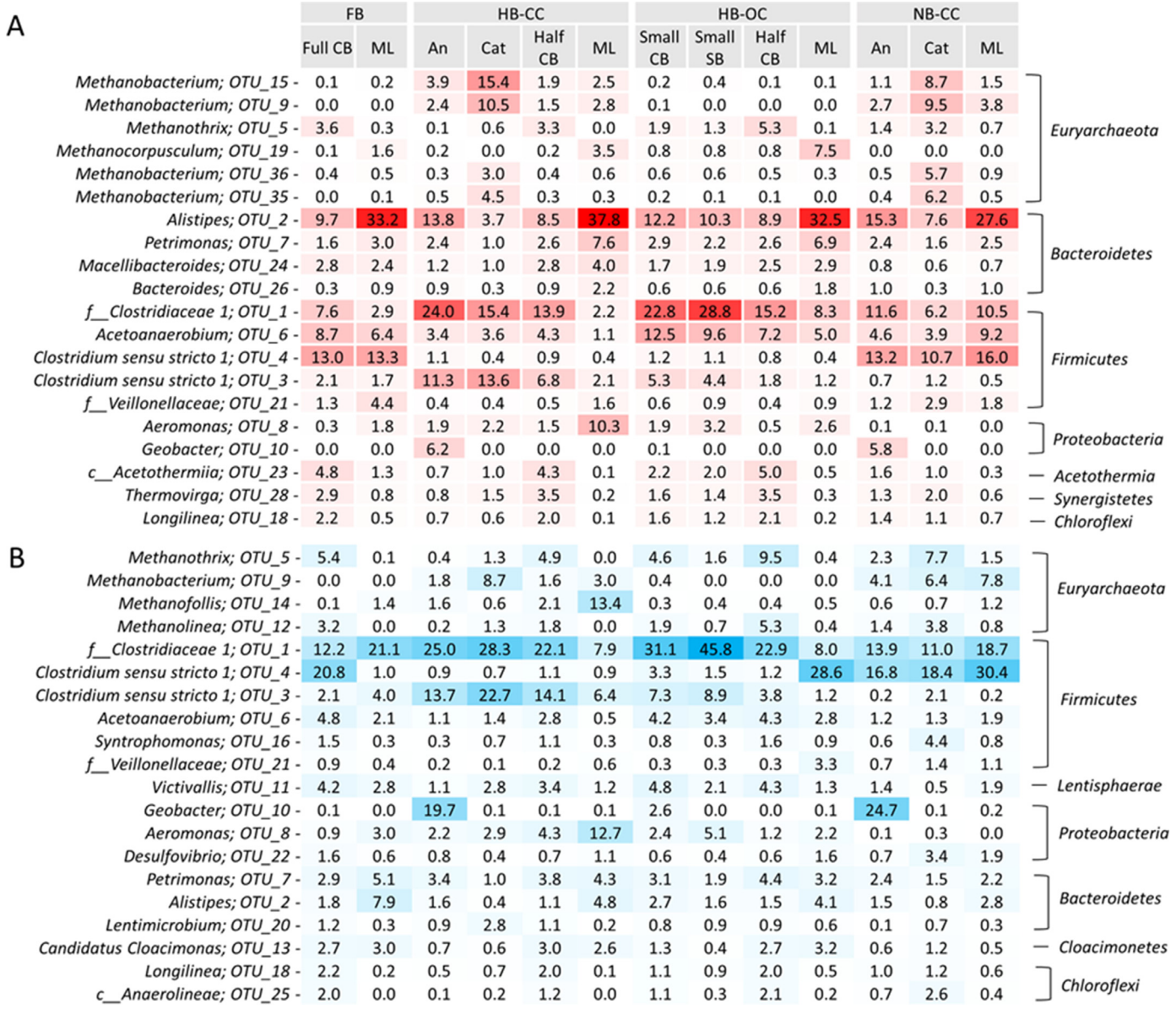

Fig. 6. Heatmap of the relative abundance (%) of top 20 dominant OTUs of microbial community structures based on (A) 16S rRNA gene and (B) 16S rRNA. The genus level or lowest taxonomic classification (f: family, c: class) possible are shown in the left column and the phylum level classification are shown in the right column. (CB; carbon brush, ML; mixed liquor, An; anode, Cat; cathode, SB; stainless steel brush).

siders rare OTUs (Ragab et al., 2019). Both indices were generally higher in large- and small-size open-circuit brushes compared to the electrode samples (Fig. S4), suggesting that more diverse functional microbial groups flourished due to the electrically conductive fibers in the brushes.

3.6. Overall analysis

Overall, the experimental results indicated that the large surface area of carbon brush was more beneficial than current generation in terms of total biogas production and rates of organic matter degradation. The enhanced performance by the AD reactors with the half or full-sized brushes (FB, HB-CC, and HB-OC reactors) was likely due to at least two reasons. First, the half- or full-size brush provided a large supporting medium, due to the higher surface area than that of the smaller brush electrodes, for attached biomass. In comparison to a suspended growth system, attached growth is known to sustain more biomass inside the reactors and thus to provide greater biological stability and efficiency of COD removal (Rajeshwari et al., 2000). Second, the carbon brushes used in this study were electrically conductive (650 S/cm; zoltek.com/products/px35) so the brush fibers could have promoted DIET between electroactive VFA-degrading bacteria and methanogens consistent with previous reports using electrically conductive materials (Rotaru et al., 2014a; Rotaru et al., 2014b). Several other studies have also shown enhanced AD efficiency by DIET stimulation by adding conductive carbon-based materials (Chen et al., 2014; Dang et al., 2016; Zhao et al., 2017; Zhao et al., 2015). The addition of conductive materials improved, for example, methane production and the degradation rate of acetate (Kato et al., 2012), propionate (Jing et al., 2017), and butyrate (Li et al., 2015) in mixed-culture AD process, which were the major VFAs in the present study. Considering that half- and full-size carbon brushes can provide very large conductive surface areas for microorganisms to be attached, both beneficial effects (i.e., large area for attached growth and increased DIET) might be achieved

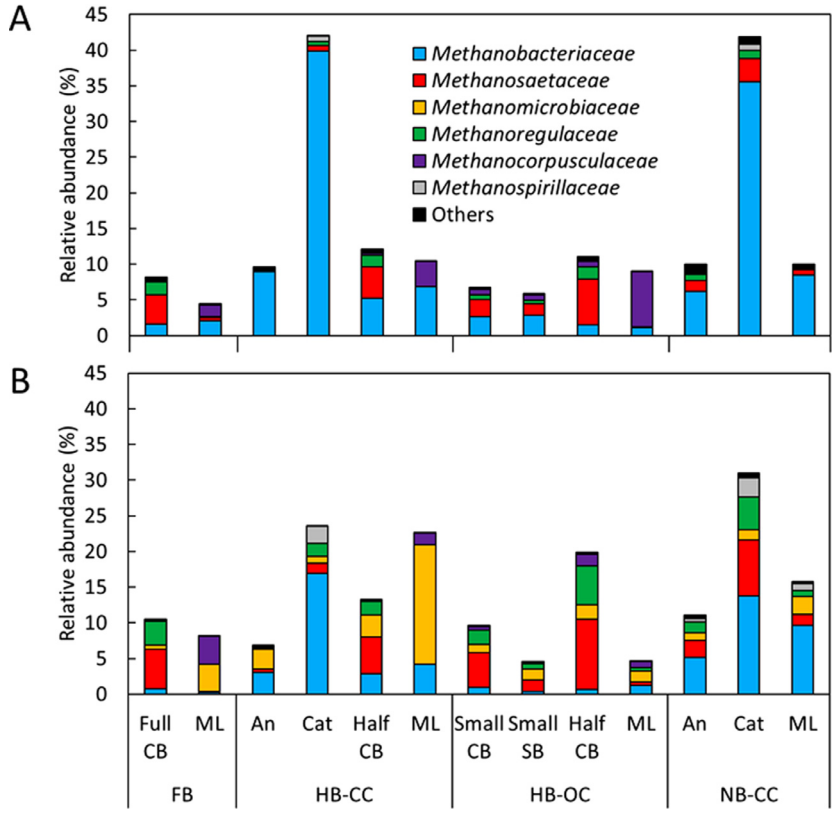

Fig. 7. The relative abundance of methanogenic community at the family level based on (A) 16S rRNA gene and (B) 16S rRNA. The community with relative abundance < 1% of the sequence reads in any sample or was not assigned to any family level was classified as "Others". (CB; carbon brush, ML; mixed liquor, An; anode, Cat; cathode, SB; stainless steel brush).

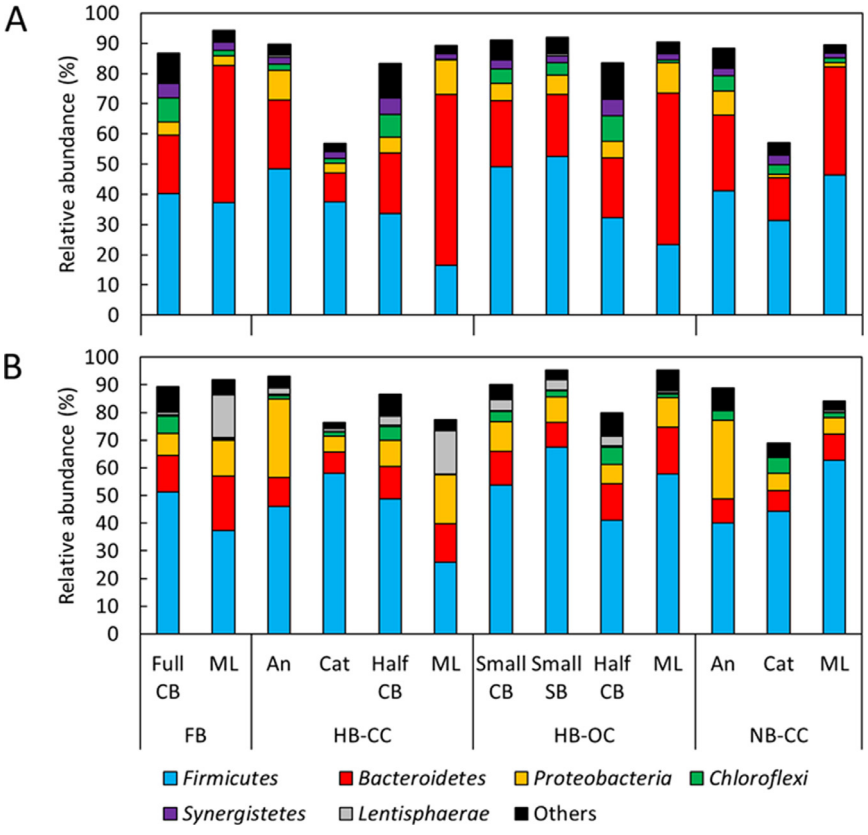

Fig. 8. The relative abundance of bacterial community at the phylum level based on (A) 16S rRNA gene and (B) 16S rRNA. The community with relative abundance < 5% of the sequence reads in any sample or was not assigned to any phylum level was classified as "Others". (CB; carbon brush, ML; mixed liquor, An; anode, Cat; cathode, SB; stainless steel brush).

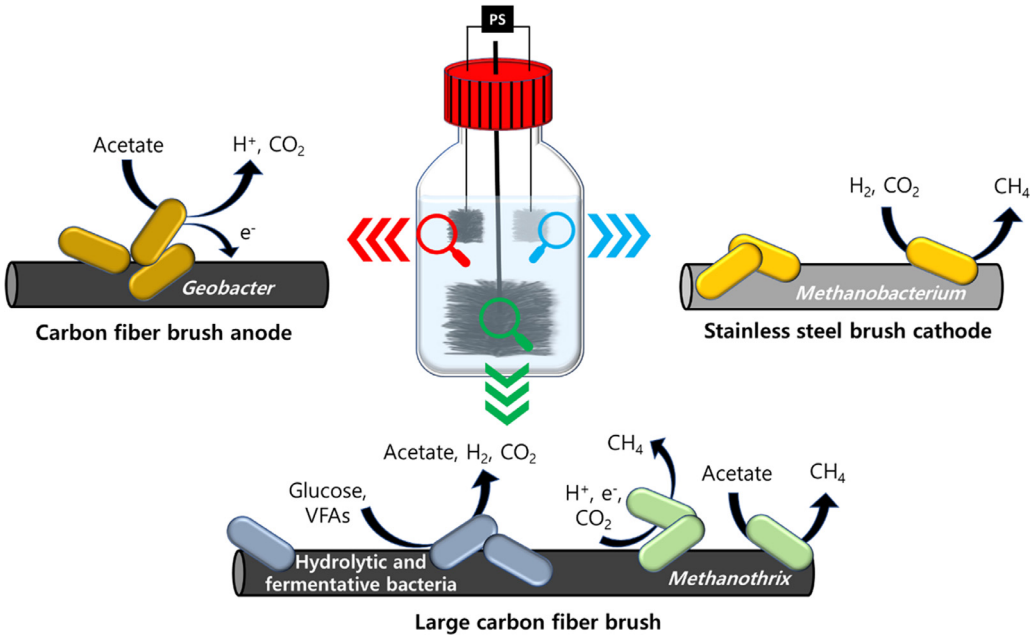

Fig. 9. Schematic describing the major microbial activity occurring in each carbon fiber brush anode, stainless steel brush cathode, and large carbon fiber brush.

in the reactors with relatively large brushes. Based on chemical and microbial community results, a potential schematic was presented to describe the major microbial activity occurring in each biofilm on the brush (Fig. 9). The presence of large carbon brush was the main factor in improving AD performance, with *Methanothrix*, dominant methanogen in carbon brush, possibly responsible for the improved performance.

The more critical impact of surface area than current generation observed here suggests that the role of bioelectrodes in AD-MEC systems should be reconsidered in terms of their impact. In some AD-MEC studies the contribution of current to overall methane production (i.e. $r_{th/tot}$ values) was quite low, for example 0.6% (Feng et al., 2015) and <1.2% (Baek et al., 2020). The $r_{th/tot}$ values here were 2.9% (HB-CC) and 7.7% (NB-CC), which was larger than in these previous studies but apparently still too low to produce differences in methane production efficiency among reactors with electrodes. The common factor in the reactor configuration for these three studies (Baek et al., 2020; Feng et al., 2015 and this study) was a low electrode packing density (0.6–0.7 m^2/m^3 based on the cathode projected area to reactor volume). This indicated that current generation was not the only factor to enhance methane productivity or the stability of AD operation in previous studies. Rather than current, high biomass concentration on the large electrode surface with less washout effect could make a major contribution to methane production. Consistent with this observation was the fact that there was no significant difference in AD-MEC performance observed between closed and open circuit in the presence of electrodes in previous study (De Vrieze et al., 2014). As an extension of our results, we suggest that enhanced AD can be achieved simply by maximizing the surface area through addition of large graphite fiber brushes, rather than by adding electrodes with current generation.

4. Conclusions

The addition of a large amount of conductive surface area using carbon brush was proved to be more efficient for AD performance than current generation through electrodes. FB, HB-CC, and HB-OC showed 57-82% higher methane generation rate parameters in the Gompertz model compared to the NB-CC, as well as the enhancement in VFA removals. Much higher amounts of protein in the large-size brushes and negligible impact of current production on the CH_4 production were observed, suggesting a more important role of adding large surface area than producing current. *Methanothrix* was the dominant methanogen on the large-size carbon brush, while *Geobacter* (anode) and *Methanobacterium* (cathode) were most abundant on the electrodes. These results highlight that providing surface area by using electrically conductive carbon fiber brushes could be a better strategy for enhancing AD performance than using only MEC electrodes with an applied potential.

Conflict of interest statement

The authors certify that they have NO affiliations with or involvement in any organization or entity with any financial interest (such as honoraria; educational grants; participation in speakers' bureaus; membership, employment, consultancies, stock ownership, or other equity interest; and expert testimony or patent-licensing arrangements), or non-financial interest (such as personal or professional relationships, affiliations, knowledge or beliefs) in the subject matter or materials discussed in this manuscript.

Declaration of Competing Interest

The authors declare that they have no known competing financial interests or personal relationships that could have appeared to influence the work reported in this paper.

Acknowledgements

This research was funded by the Stan and Flora Kappe endowment and other funds through The Pennsylvania State University.

Supplementary materials

Supplementary material associated with this article can be found, in the online version, at doi:10.1016/j.watres.2020.116575.

References

Apprill, A., McNally, S., Parsons, R., Weber, L., 2015. Minor revision to V4 region SSU rRNA 806R gene primer greatly increases detection of SAR11 bacterioplankton. Aquat. Microb. Ecol. 75 (2), 129–137.

Association, A.P.H., Association, A.W.W., Federation, W.P.C., Federation, W.E., 1920. Standard methods for the examination of water and wastewater. American Public Health Association.

Baek, G., Kim, J., Cho, K., Bae, H., Lee, C., 2015. The biostimulation of anaerobic digestion with (semi) conductive ferric oxides: their potential for enhanced biomethanation. Appl. Microbiol. Biotechnol. 99 (23), 10355–10366.

Baek, G., Kim, J., Kim, J., Lee, C., 2018. Role and potential of direct interspecies electron transfer in anaerobic digestion. Energies 11 (1), 107.

Baek, G., Kim, J., Kim, J., Lee, C., 2020. Individual and combined effects of magnetite addition and external voltage application on anaerobic digestion of dairy wastewater. Bioresour. Technol. 297, 122443.

Baek, G., Kim, J., Lee, S., Lee, C., 2017. Development of biocathode during repeated cycles of bioelectrochemical conversion of carbon dioxide to methane. Bioresour. Technol. 241, 1201–1207.

Bond, D.R., Lovley, D.R., 2003. Electricity production by Geobacter sulfurreducens attached to electrodes. Appl. Environ. Microbiol. 69 (3), 1548–1555.

Cai, W., Liu, W., Yang, C., Wang, L., Liang, B., Thangavel, S., Guo, Z., Wang, A., 2016. Biocathodic methanogenic community in an integrated anaerobic digestion and microbial electrolysis system for enhancement of methane production from waste sludge. ACS Sustainable Chem. Eng. 4 (9), 4913–4921.

Cario, B.P., Rossi, R., Kim, K.-Y., Logan, B.E., 2019. Applying the electrode potential slope method as a tool to quantitatively evaluate the performance of individual microbial electrolysis cell components. Bioresour. Technol. 287, 121418.

Chen, C., Yao, X., Li, Q.X., Wang, Q., Liang, J., Zhang, S., Ming, J., Liu, Z., Deng, J., Yoza, B.A., 2018. Turf soil enhances treatment efficiency and performance of phenolic wastewater in an up-flow anaerobic sludge blanket reactor. Chemosphere 204, 227–234.

Chen, S., Rotaru, A.-E., Liu, F., Philips, J., Woodard, T.L., Nevin, K.P., Lovley, D.R., 2014. Carbon cloth stimulates direct interspecies electron transfer in syntrophic co–cultures. Bioresour. Technol. 173, 82–86.

Cheng, S., Xing, D., Call, D.F., Logan, B.E., 2009. Direct biological conversion of electrical current into methane by electromethanogenesis. Environ. Sci. Technol. 43 (10), 3953–3958.

Choong, Y.Y., Chou, K.W., Norli, I., 2018. Strategies for improving biogas production of palm oil mill effluent (POME) anaerobic digestion: A critical review. Renewable Sustainable Energy Rev 82, 2993–3006.

Cruz Viggi, C., Rossetti, S., Fazi, S., Paiano, P., Majone, M., Aulenta, F., 2014. Magnetite particles triggering a faster and more robust syntrophic pathway of methanogenic propionate degradation. Environ. Sci. Technol. 48 (13), 7536–7543.

Dang, Y., Holmes, D.E., Zhao, Z., Woodard, T.L., Zhang, Y., Sun, D., Wang, L.-Y., Nevin, K.P., Lovley, D.R., 2016. Enhancing anaerobic digestion of complex organic waste with carbon-based conductive materials. Bioresour. Technol. 220, 516–522.

De Vrieze, J., Devooght, A., Walraedt, D., Boon, N., 2016. Enrichment of Methanosaetaceae on carbon felt and biochar during anaerobic digestion of a potassium-rich molasses stream. Appl. Microbiol. Biotechnol. 100 (11), 5177–5187.

De Vrieze, J., Gildemyn, S., Arends, J.B., Vanwonterghem, I., Verbeken, K., Boon, N., Verstraete, W., Tyson, G.W., Hennebel, T., Rabaey, K., 2014. Biomass retention on electrodes rather than electrical current enhances stability in anaerobic digestion. Water Res 54, 211–221.

Ding, A., Yang, Y., Sun, G., Wu, D., 2016. Impact of applied voltage on methane generation and microbial activities in an anaerobic microbial electrolysis cell (MEC). Chem. Eng. J. 283, 260–265.

Feng, Q., Song, Y.-C., Ahn, Y., 2018. Electroactive microorganisms in bulk solution contribute significantly to methane production in bioelectrochemical anaerobic reactor. Bioresour. Technol. 259, 119–127.

Feng, Y., Zhang, Y., Chen, S., Quan, X., 2015. Enhanced production of methane from waste activated sludge by the combination of high-solid anaerobic digestion and microbial electrolysis cell with iron–graphite electrode. Chem. Eng. J. 259, 787–794.

Illumina, I. 2015. 16S metagenomic sequencing library preparation. Part# 15044223 Rev. B.

Ishii, S.i., Watanabe, K., Yabuki, S., Logan, B.E., Sekiguchi, Y., 2008. Comparison of electrode reduction activities of Geobacter sulfurreducens and an enriched consortium in an air-cathode microbial fuel cell. Appl. Environ. Microbiol. 74 (23), 7348–7355.

Jing, Y., Wan, J., Angelidaki, I., Zhang, S., Luo, G., 2017. iTRAQ quantitative proteomic analysis reveals the pathways for methanation of propionate facilitated by magnetite. Water Res 108, 212–221.

Kang, H., Jeong, J., Gupta, P.L., Jung, S.P., 2017. Effects of brush-anode configurations on performance and electrochemistry of microbial fuel cells. Int. J. Hydrogen Energy 42 (45), 27693–27700.

Kato, S., Hashimoto, K., Watanabe, K., 2012. Methanogenesis facilitated by electric syntrophy via (semi) conductive iron-oxide minerals. Environ. Microbiol. 14 (7), 1646–1654.

Li, H., Chang, J., Liu, P., Fu, L., Ding, D., Lu, Y., 2015. Direct interspecies electron transfer accelerates syntrophic oxidation of butyrate in paddy soil enrichments. Environ. Microbiol. 17 (5), 1533–1547.

Lin, P.-Y., Whang, L.-M., Wu, Y.-R., Ren, W.-J., Hsiao, C.-J., Li, S.-L., Chang, J.-S., 2007. Biological hydrogen production of the genus Clostridium: metabolic study and mathematical model simulation. Int. J. Hydrogen Energy 32 (12), 1728–1735.

Liu, C., Yuan, X., Gu, Y., Chen, H., Sun, D., Li, P., Li, M., Dang, Y., Smith, J.A., Holmes, D.E., 2020a. Enhancement of bioelectrochemical CO2 reduction with carbon brush electrode via direct electron transfer. ACS Sustainable Chem. Eng. 8 (30), 11368–11375.

Liu, F., Rotaru, A.-E., Shrestha, P.M., Malvankar, N.S., Nevin, K.P., Lovley, D.R., 2012. Promoting direct interspecies electron transfer with activated carbon. Energy Environ. Sci. 5 (10), 8982–8989.

Liu, W., Cai, W., Guo, Z., Wang, L., Yang, C., Varrone, C., Wang, A., 2016. Microbial electrolysis contribution to anaerobic digestion of waste activated sludge, leading to accelerated methane production. Renewable Energy 91, 334–339.

Liu, X., Chen, Q., Sun, D., Wang, Y., Dong, H., Dang, Y., Holmes, D.E., 2020b. Applying potentials to conductive materials impairs high-loading anaerobic digestion performance by affecting direct interspecies electron transfer. Bioresour. Technol. 297, 122422.

Logan, B., Cheng, S., Watson, V., Estadt, G., 2007. Graphite fiber brush anodes for increased power production in air-cathode microbial fuel cells. Environ. Sci. Technol. 41 (9), 3341–3346.

Lu, J.-H., Chen, C., Huang, C., Zhuang, H., Leu, S.-Y., Lee, D.-J., 2020. Dark fermentation production of volatile fatty acids from glucose with biochar amended biological consortium. Bioresour. Technol. 303, 122921.

Nam, T., Son, S., Koo, B., Tran, H.V.H., Kim, J.R., Choi, Y., Jung, S.P., 2017. Comparative evaluation of performance and electrochemistry of microbial fuel cells with different anode structures and materials. Int. J. Hydrogen Energy 42 (45), 27677–27684.

Pampillón-González, L., Ortiz-Cornejo, N.L., Luna-Guido, M., Dendooven, L., Navarro-Noya, Y.E., 2017. Archaeal and bacterial community structure in an anaerobic digestion reactor (Lagoon Type) used for biogas production at a pig farm. J. Mol. Microbiol. Biotechnol. 27 (5), 306–317.

Qin, Y., Yin, X., Xu, X., Yan, X., Bi, F., Wu, W., 2020. Specific surface area and electron donating capacity determine biochar's role in methane production during anaerobic digestion. Bioresour. Technol. 303, 122919.

Ragab, A., Katuri, K., Ali, M., Saikaly, P.E., 2019. Evidence of spatial homogeneity in an electromethanogenic cathodic microbial community. Front. Microbiol. 10, 1747.

Rajeshwari, K., Balakrishnan, M., Kansal, A., Lata, K., Kishore, V., 2000. State-of-the-art of anaerobic digestion technology for industrial wastewater treatment. Renewable Sustainable Energy Rev 4 (2), 135–156.

Rossi, R., Yang, W., Zikmund, E., Pant, D., Logan, B.E., 2018. In situ biofilm removal from air cathodes in microbial fuel cells treating domestic wastewater. Bioresour. Technol. 265, 200–206.

Rotaru, A.-E., Shrestha, P.M., Liu, F., Markovaite, B., Chen, S., Nevin, K.P., Lovley, D.R., 2014a. Direct interspecies electron transfer between Geobacter metallireducens and Methanosarcina barkeri. Appl. Environ. Microbiol 80 (15), 4599–4605.

Rotaru, A.-E., Shrestha, P.M., Liu, F., Shrestha, M., Shrestha, D., Embree, M., Zengler, K., Wardman, C., Nevin, K.P., Lovley, D.R., 2014b. A new model for electron flow during anaerobic digestion: direct interspecies electron transfer to Methanosaeta for the reduction of carbon dioxide to methane. Energy Environ. Sci. 7 (1), 408–415.

Show, K.-Y., Tay, J.-H., 1999. Influence of support media on biomass growth and retention in anaerobic filters. Water Res 33 (6), 1471–1481.

Siegert, M., Yates, M.D., Spormann, A.M., Logan, B.E., 2015. Methanobacterium dominates biocathodic archaeal communities in methanogenic microbial electrolysis cells. ACS Sustainable Chem. Eng. 3 (7), 1668–1676.

Sposob, M., Moon, H.-S., Lee, D., Kim, T.-H., Yun, Y.-M., 2020. Comprehensive analysis of the microbial communities and operational parameters of two full-scale anaerobic digestion plants treating food waste in South Korea: seasonal variation and effect of ammonia. J. Hazard. Mater., 122975.

Suarez, E.M., Lepkova, K., Kinsella, B., Machuca, L.L., 2019. Aggressive corrosion of steel by a thermophilic microbial consortium in the presence and absence of sand. Int. Biodeterior. Biodegrad. 137, 137–146.

Trzcinski, A.P., Stuckey, D.C., 2012. Determination of the hydrolysis constant in the biochemical methane potential test of municipal solid waste. Environ. Eng. Sci. 29 (9), 848–854.

Vu, M.T., Noori, M.T., Min, B., 2020. Conductive magnetite nanoparticles trigger syntrophic methane production in single chamber microbial electrochemical systems. Bioresour. Technol. 296, 122265.

Xu, Y., Wang, M., Yu, Q., Zhang, Y., 2020. Enhancing methanogenesis from anaerobic digestion of propionate with addition of Fe oxides supported on conductive carbon cloth. Bioresour. Technol. 302, 122796.

Yu, Z., Leng, X., Zhao, S., Ji, J., Zhou, T., Khan, A., Kakde, A., Liu, P., Li, X., 2018. A review on the applications of microbial electrolysis cells in anaerobic digestion. Bioresour. Technol. 255, 340–348.

Zhang, J., Zhang, R., Wang, H., Yang, K., 2020. Direct interspecies electron transfer stimulated by granular activated carbon enhances anaerobic methanation efficiency from typical kitchen waste lipid-rapeseed oil. Sci. Tot. Environ. 704, 135282.

Zhang, J., Zhang, Y., Quan, X., Chen, S., Afzal, S., 2013. Enhanced anaerobic digestion of organic contaminants containing diverse microbial population by combined microbial electrolysis cell (MEC) and anaerobic reactor under Fe(III) reducing conditions. Bioresour. Technol. 136, 273–280.

Zhao, Z., Li, Y., Yu, Q., Zhang, Y., 2018. Ferroferric oxide triggered possible direct interspecies electron transfer between Syntrophomonas and Methanosaeta to enhance waste activated sludge anaerobic digestion. Bioresour. Technol. 250, 79–85.

Zhao, Z., Zhang, Y., Li, Y., Dang, Y., Zhu, T., Quan, X., 2017. Potentially shifting from interspecies hydrogen transfer to direct interspecies electron transfer for syntrophic metabolism to resist acidic impact with conductive carbon cloth. Chem. Eng. J. 313, 10–18.
Zhao, Z., Zhang, Y., Quan, X., Zhao, H., 2016. Evaluation on direct interspecies electron transfer in anaerobic sludge digestion of microbial electrolysis cell. Bioresour. Technol. 200, 235–244.
Zhao, Z., Zhang, Y., Woodard, T., Nevin, K., Lovley, D., 2015. Enhancing syntrophic metabolism in up-flow anaerobic sludge blanket reactors with conductive carbon materials. Bioresour. Technol. 191, 140–145.
Zhen, G., Lu, X., Kobayashi, T., Kumar, G., Xu, K., 2016. Promoted electromethanosynthesis in a two-chamber microbial electrolysis cells (MECs) containing a hybrid biocathode covered with graphite felt (GF). Chem. Eng. J. 284, 1146–1155.
Zoetendal, E.G., Plugge, C.M., Akkermans, A.D., de Vos, W.M., 2003. Victivallis vadensis gen. nov., sp. nov., a sugar-fermenting anaerobe from human faeces. Int. J. Syst. Evol. Microbiol. 53 (1), 211–215.